Magnetic nanoconstructions of iron oxides coated with arabinogalactan functionalized with DNA aptamer

Magnetic nanoconstructions of iron oxides coated with arabinogalactan functionalized with DNA aptamer

S V Stolyar[1,2,3], L A Chekanova[2], R N Yaroslavtsev[1,2,3], S V Komogortsev[2], Yu V Gerasimova[2], O A Bayukov[2], M N Volochaev[2], R S Iskhakov[2], I V Garanzha[3], O S Kolovskaya[3,4], M Sh Bairmani[5,6] and T N Zamay[4]

[1] Siberian Federal University, Krasnoyarsk, Russia
[2] Kirensky Institute of Physics, Federal Research Center KSC SB RAS, Krasnoyarsk, Russia
[3] Krasnoyarsk Scientific Center, Federal Research Center KSC SB RAS Krasnoyarsk, Russia
[4] Krasnoyarsk State Medical University named after prof. V.F. Voino-Yasenecki, Krasnoyarsk, 660022, Russia
5Astrakhan State University, Tatisheva 20 A, Astrakhan, 414056, Russia
[6] College of Biotechnology, Al-Qasim Green University, Iraq

E-mail: Stol@iph.krasn.ru

Abstract. New composite nanoparticles for biomedical applications have been manufactured. The particles consist of an anisomeric magnetite core coated with arabinogalactan and are functionalized with cameras for As-14 ascites cells (Ehrlich carcinoma). The binding of ascitic Ehrlich carcinoma cells to magnetic nanoparticles was evaluated using fluorescence microscopy.

1. Introduction

At present, oligonucleotides acting as artificial antibodies called aptamers are used as drugs for personalized medicine. Aptamers are fragments of single-stranded RNA or DNA (30-80 nucleotides). The spatial arrangement of charged phosphates and unpaired bases in the oligonucleotide determines the ability of aptamers to specific binding [1]. Due to its unique conformation, aptamer can be connected with any biological target, which allows them to be used as effective diagnostic and therapeutic drugs [2]. Polysaccharides obtained from animal, plant raw materials and from microorganisms which are environmentally friendly materials and they have widely used in medicine. Magnetic nanobiocomposites based on polysaccharides have a synergistic property of the stabilizing polysaccharide matrix and magnetic core [3]. This work was carried out to create magnetic Iron Oxides nanoparticles coated with a polysaccharide shell, to study the structure and magnetic properties of these nanoparticles with the aim of manufacturing hybrid structures equipped with DNA aptamers with the intention of provide targeted binding of the prepared composites to Ehrlich ascites carcinoma cells.

2. Experimental part

Magnetic nanoparticles were obtained by chemical deposition. As a result of the reaction of the $FeSO_4$ Iron salt and the natural water-soluble arabinogalactan polysaccharide [4], a black precipitate formed. Subsequently, the precipitate was washed with a neutral pH and dried. Structural studies were performed by X-ray phase analysis ($\lambda = 1.54$ Å) and Transmission Electron Microscopy. The magnetic properties were studied by Ferromagnetic Resonance at a frequency of f = 9 GHz. Mossbauer measurements were carried out at room temperature on an MS-1104Em spectrometer with a Co^{57} (Cr) source on powder absorbers with a thickness of 5-10 mg / cm^2 based on the natural Iron content. The obtained powders were studied by IR spectroscopy on a Vertex 70 spectrometer (Bruker) in the wave vector range of 370–7500 cm^{-1} and a resolution of 1 cm^{-1}. Samples for analysis were prepared in the form of tablets in a KBr matrix. Before functionalization, the aptameramine nanoparticles were subjected to ultrasonic treatment. Phosphate buffer, aptamers for As-14 ascitic cells and aptamer-labeled with a fluorescent FAM tag were added to the naoparticles. The binding of ascitic Ehrlich carcinoma cells to fabricated magnetic composites was determined using fluorescence microscopy.

3. Experimental results

The images obtained by transmission electron microscopy (figure 1) shows that the nanoparticles are nanocrystals in the form of plates with an average size of about 25 nm. The recording reflections of micro diffraction shown in figure 1, as well as on X-ray diffraction patterns of dried powders, can belong to maghemite (γ-Fe_2O_3) and magnetite (Fe_3O_4).

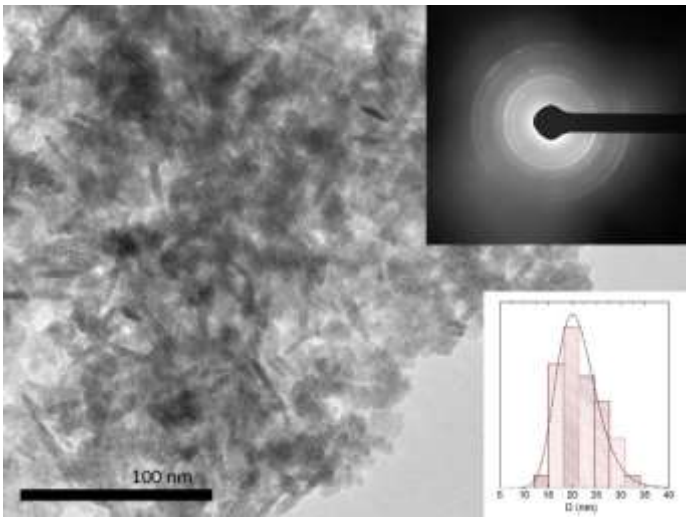

Figure 1. TEM-images of nanoparticles coated with Arabinogalactan and micro diffraction pattern and particle size distribution (on insets).

The resonance absorption curve when measuring the FMR was characterized at room temperature by a single absorption with a resonance field Hp ≈ 2900 Э, and a line width ΔH = 1600Э. To determine the Magnetization M of the obtained powders, a reference was used — magnetite powder Fe_3O_4 with M (Fe_3O_4) = 450 G. The area under the integrated microwave absorption curve is proportional to the mass of the sample and magnetization. A comparison of the resonance curves of the obtained powders and the standard allowed us to determine the M of the studied powders, which was ~ 300 G. The Mossbauer spectrum was well approximated by four Zeeman sextets. The decoding result is summarized in table 1, in which A and B denote the tetrahedral and octahedral positions of ferrite.

Table 1. Mossbauer particle parameters. IS is the isomeric chemical shift relative to α-Fe, H is the hyperfine field on the iron core, QS is the quadrupole splitting, W is the width of the absorption lines

for the internal 34 and external 16 lines of the network, P is the fractional occupancy of the position (area under partial spectrum), A is the tetrahedral and B is the octahedral position of the spinel.

IS, мм/с ± 0.01	H, кe ± 5	QS, мм/с ± 0.02	W_{34-16}, мм/с ± 0.02	P, val.% ± 0.03	Position
0.28	483	-0.01	0.36-0.36	0.24	Fe^{3+}(A) magnetite
0.56	452	-012	0.52-0.85	0.46	$Fe^{2.5+}$(B) magnetite
0.42	407	0.17	0.71-1.37	0.16	Fe^{3+}(B) magnetite
0.39	195	-0.11	0.74-4.16	0.14	Fe^{3+}(6)

Figure 2 shows the IR spectra of the used arabinogalactan powder and dried magnetic nanoparticles coated with arabinogalactan.

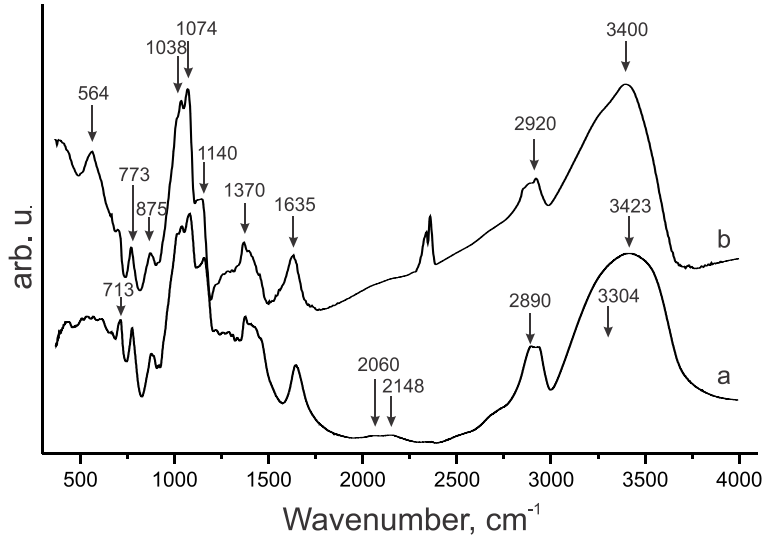

Figure 2. IR spectra a) arabinogalactan powder, b) magnetic nanoparticles coated with arabinogalactan.

After a qualitative analysis of the IR spectra of the studied samples, the main characteristic frequencies were determined, which are presented in table 2.

Table 2. Absorption bands in the IR spectra of the samples.

Spectral region, cm^{-1}	Maximum absorption band, cm^{-1} arabinagalactan powder	Maximum absorption band, cm^{-1} magnetic nanoparticles coated with arabinogalactan	Assignment of absorption bands
370–600		564	Fe-O stretching
	713	704	The range of vibrations of the pyranose ring and the deformation vibrations of hydroxyl groups
	774	773	
800–1000	875	875	C-O-C link oscillations + deformation vibrations CH_2

1000–1200	1038 1077 1148	1038 1074 1140	C-O stretching, internal vibrations of C – O bonds, (bands characteristic of polysaccharides (due to the presence of acetal bonds
1200–1500	1370	1370	deformation vibrations of the C-H bond
1500–2000	1640	1635	deformational vibrations of bonds in H – O – H (adsorbed water) 1635cm-^{1}
2000–3000	2060 2148 2890 2920	 2890 2920	internal vibrations of bonds in the groups CH and CH_2 C-H
3000–4000	3423	3400	internal vibrations of HO groups participating in intermolecular and intramolecular H bonds (unresolved (structure

In the spectra of both samples (figure 2), the most intense vibrations of the hydroxyl group are at ν = 3400 cm $^{-1}$. All hydroxyl groups are involved in hydrogen bonds since The IR absorption of free hydroxyl groups is ~ 3650 cm $^{-1}$. As a rule, the band at 2920 cm $^{-1}$ (νC – H) is used as a comparison if the number of C – H valence bonds does not change in a number of studied samples. In the region of 1635 cm $^{-1}$, adsorbed water molecules absorb. With increasing water content, the maximum shifts somewhat toward large wave numbers. The 1370 cm $^{-1}$ band characterizes the deformation vibrations of the C – H bonds. The intense band at 1074 cm $^{-1}$ in both compounds refers to the stretching of CO bonds. All frequencies of intense vibrations are shown in the table. The spectrum of the dried sol of magnetic particles differs from the spectrum of a dry powder of arabinogalactan in the region of 500 cm^{-1}, the vibration of 564 cm^{-1} refers to the stretching modes of Fe-O iron oxides, by the appearance of this vibration we can talk about the formation of a bond between magnetic nanoparticles of iron oxides and arabinogalactan.

4. Study of the binding of magnetic nanoparticles to ascitic Ehrlich carcinoma cells

The isolation of ascites cells was performed on the 9th day after tumor transplantation. To do this, ascites was taken from the abdominal cavity of mice, which was centrifuged for 5 minutes at 5 thousand rpm. The collected cells were washed three times in phosphate buffer containing calcium and magnesium. Cells were diluted with phosphate buffer in a 1: 1 ratio (cells, phosphate buffer). Before functionalization, the nanoparticles were subjected to ultrasound to reduce aggregates. After that, 50 μl of 2-fold phosphate buffer, aptamers to As-14 ascites cells (final concentration of aptamer 0.5 μM) and fluorescent FAM tag As-42 aptamers (final concentration of aptamer 0.5 μM) were added to 50 μl of a suspension of nanoparticles) The resulting mixture was incubated on a shaker at room temperature for 30 minutes. Magnetic separation was used to separate unbound nanoparticles and aptamers, resulting in nanoparticles bound to aptamers to ascites cells and aptamers with a fluorescent dye. Then, to 100 μl of a suspension of nanoparticles functionalized by anamers, 40 μl of Ehrlich carcinoma cells were added and incubated for 30 minutes. Figure 3 shows photographs of ascites cells associated with magnetic nanoparticles obtained using light microscopy (a) and fluorescence microscopy (b). Cells associated with the fabricated constructs were fluorescent.

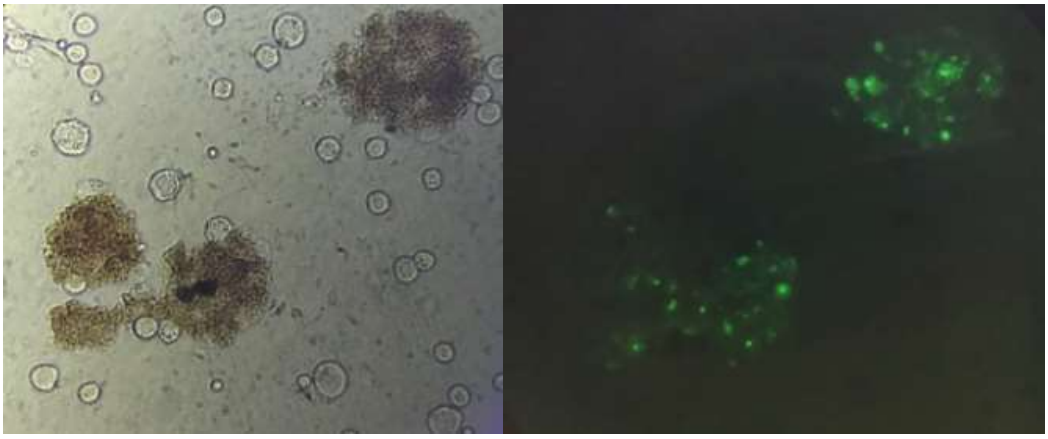

Figure 3. Photos of ascites cells associated with magnetic nanoparticles obtained using light microscopy and fluorescence microscopy.

5. Discussion

By chemical precipitation, salts of magnetic nanoparticles of Fe oxides in an aqueous solution of arabinogalactan were obtained. The use of this polysaccharide is due to its biocompatibility. Structural studies did not allow us to uniquely identify the phase composition of the fabricated nanoparticles. Comparative measurements carried out by IR spectroscopy of dried sols of magnetic nanoparticles and the arabinogalactan powder used, namely, the detected vibration at 564 cm^{-1}, indicate the formation of a bond between the magnetic nanoparticles of iron oxides and the polysaccharide. Information on the phase composition was obtained using Mössbauer spectroscopy (see table 1). The widths of the lines of the octahedral positions are rather broadened, which may indicate an inhomogeneous distribution of heterovalent cations over these positions. The positions designated as Fe_3 + (6) can be attributed to near-surface positions with a strong fluctuation of the local environment. The presence of Fe ions of mixed valence $Fe^{2.5+,}$ IS = 0.56 mm / s, indicates that we are dealing with magnetite. Assuming there is no substitution of iron for other cations and perfect anionic lattice, the Mössbauer data allow us to write the spinel formula under conditions of its electroneutrality: $(Fe^{3+})[Fe^{2+}_{0.658}Fe^{3+}_{1.228}\square_{0.114}]O_4$ where □ means cationic vacancy. In this approximation, we are dealing with cation-deficient magnetite. In principle, such a system can be called a solid solution of magnetite Fe_3O_4 and maghemite γ-Fe_2O_3. The magnetization of the fabricated nanoparticles is 300 G, which is comparable with the magnetization of Fe_3O_4 γ-Fe_2O_3. The thermal effects of nanoparticles in magnetic fields, due to the scattering of the magnetic field energy in the relaxation of the magnetic moment at frequencies of ~ 1 MHz, leads to local heating, which can be used in various problems hyperthermia. The peculiarity of the nanoparticles made by us is in their shape. Particles are plates about 5 nm thick (see figure 1). The anisotropy constant of plate-shaped nanocrystals can be estimated through the sum of the contributions of magnetic anisotropy of the form $K_{sh} = \pi M_s^2$ magnetocrystalline anisotropy of magnetite $K_u = 1.3 \cdot 10^5\ erg/cm^3$, and also the contribution of surface magnetic anisotropy ($k_s = 2.9 \cdot 10^{-2}\ erg/cm^2$) [5]. The sum of these three contributions for the nanoparticles made by us, 5 nm thick and 25 nm in diameter, exceeds the constant of spherical particles of the same volume because of the significant contribution of the magnetic anisotropy of the shape [6] and the larger contribution of the surface; therefore, more significant magnetic hysteresis should be expected in such particles, and, therefore, specific heat. The prepared nanoparticles were able to functionalize the anteamic to ascitic Ehrlich carcinoma cells and labeled with a fluorescent FAM tag. The prepared magnetic complexes were bound to ascitic cells using asialoglycoprotene receptors located on the cell membrane (ligand - galactose) and entered the cell by endocytosis. Only single nanoparticles entered the cell; conglomerates did not enter the cells. The cells into which the nanoparticles entered were fluorescent.

6. Conclusion

As a result of the chemical reaction of the $FeSO_4$ iron salt and the natural water-soluble arabinogalactan polysaccharide, magnetic magnetite powders in the form of plates with a saturation magnetization of ~ 300 G coated with arabinogalactan were synthesized. Magnetic nanoparticles were functionalized through polysaccharide DNA aptamers to Erslich and Erlich red blood cell carcinoma cells. The binding of ascitic Ehrlich carcinoma cells to magnetic nanoparticles was determined using fluorescence microscopy. The fabricated nanoconstructions are promising for applied problems of hyperthermia.

References

[1] Patel, D.J. and Suri, A.K., 2000. Structure, recognition and discrimination in RNA aptamer complexes with cofactors, amino acids, drugs and aminoglycoside antibiotics. Reviews in Molecular Biotechnology, 74(1), pp.39-60

[2] Wilson D.S., Szostak J.W.In Vitro Selection of Functional Nucleic Acids, Annual Review of Biochemistry, Volume 68, 1999, pp 611-647

[3] Uthaman, S., Lee, S.J., Cherukula, K., Cho, C.S. and Park, I.K., 2015. Polysaccharide-coated magnetic nanoparticles for imaging and gene therapy. BioMed research international, 2015

[4] Trofimov, B.A., Sukhov, B.G., Aleksandrova, G.P., Medvedeva, S.A. and Grishchenko, L.A., 2003. AG Mal'-kina, LP Feoktistova, AN Sapozhnikov, VI Dubrovina, EF Martynovich, VV Tirskii, AL Semenov. In Doklady Chem (Vol. 393, pp. 287-288)

[5] Perez, N., Guardia, P., Roca, A.G., Morales, M.D.P., Serna, C.J., Iglesias, O., Bartolome, F., Garcia, L.M., Batlle, X. and Labarta, A., 2008. Surface anisotropy broadening of the energy barrier distribution in magnetic nanoparticles. Nanotechnology, 19(47), p.475704

[6] Stolyar S V., Komogortsev S V., Chekanova L A, Yaroslavtsev R N, Bayukov O A, Velikanov D A, Volochaev M N, Cheremiskina E V., Bairmani M S, Eroshenko P E and Iskhakov R S., 2019. Magnetite Nanocrystals with a High Magnetic Anisotropy Constant due to the Particle Shape. Tech. Phys. Lett. 45, 878–81